

Serotonergic modulation of the activity of GLP-1 producing neurons in the nucleus of the solitary tract in mouse



Marie K. Holt¹, Ida J. Llewellyn-Smith², Frank Reimann³, Fiona M. Gribble³, Stefan Trapp^{1,*}

ABSTRACT

Objective: Glucagon-like peptide-1 (GLP-1) and 5-HT are potent regulators of food intake within the brain. GLP-1 is expressed by preproglucagon (PPG) neurons in the nucleus tractus solitarius (NTS). We have previously shown that PPG neurons innervate 5-HT neurons in the ventral brainstem. Here, we investigate whether PPG neurons receive serotonergic input and respond to 5-HT.

Methods: We employed immunohistochemistry to reveal serotonergic innervation of PPG neurons. We investigated the responsiveness of PPG neurons to 5-HT using *in vitro* Ca²⁺ imaging in brainstem slices from transgenic mice expressing the Ca²⁺ indicator, GCaMP3, in PPG neurons, and cell-attached patch-clamp recordings.

Results: Close appositions from 5-HT-immunoreactive axons occurred on many PPG neurons. Application of 20 μM 5-HT produced robust Ca²⁺ responses in NTS PPG dendrites but little change in somata. Dendritic Ca²⁺ spikes were concentration-dependent (2, 20, and 200 μM) and unaffected by blockade of glutamatergic transmission, suggesting 5-HT receptors on PPG neurons. Neither activation nor blockade of 5-HT₃ receptors affected [Ca²⁺]_i. In contrast, inhibition of 5-HT₂ receptors attenuated increases in intracellular Ca²⁺ and 5-HT_{2C} receptor activation produced Ca²⁺ spikes. Patch-clamp recordings revealed that 44% of cells decreased their firing rate under 5-HT, an effect blocked by 5-HT_{1A} receptor antagonism.

Conclusions: PPG neurons respond directly to 5-HT with a 5-HT_{2C} receptor-dependent increase in dendritic [Ca²⁺]_i. Electrical responses to 5-HT revealed additional inhibitory effects due to somatic 5-HT_{1A} receptors. Reciprocal innervation between 5-HT and PPG neurons suggests that the coordinated activity of these brainstem neurons may play a role in the regulation of food intake.

© 2017 The Authors. Published by Elsevier GmbH. This is an open access article under the CC BY license (<http://creativecommons.org/licenses/by/4.0/>).

Keywords Serotonin; Preproglucagon; GCaMP; Dendritic calcium; NTS

1. INTRODUCTION

Glucagon-like peptide-1 (GLP-1) is an incretin best known for its role in glucose homeostasis and appetite regulation [1]. Activation of brain GLP-1 receptors also increases heart rate and blood pressure, induces nausea, and activates the hypothalamic–pituitary–adrenal (HPA) axis in both humans and rodents [2–5]. Along with reduced appetite, activation of the sympathetic nervous system and the HPA axis are both symptoms of stress; and stress-induced hypophagia has recently been shown to depend partly on activation of brain GLP-1 receptors [6–8]. Within the brain, GLP-1 is produced by preproglucagon (PPG) neurons in the lower brainstem [9–12]. These neurons are ideally situated to receive information about homeostatic stress and energy balance from the rest of the body. Gastric distention and cholecystokinin, both peripheral signals of satiety, induce expression of the immediate early

gene *c-fos* in GLP-1-expressing neurons, suggesting PPG neurons could play a role in relaying peripheral satiety signals [13,14]. Indeed, chemogenetic activation of PPG neurons has recently been shown to induce hypophagia and body weight loss, suggesting these neurons have the potential to regulate food intake [15]. PPG neurons project from the nucleus of the solitary tract (NTS) and intermediate reticular nucleus (IRT) to autonomic control centers throughout the central nervous system, including sympathetic preganglionic neurons in the spinal cord [9,16]. Many of these nuclei have been shown to express GLP-1 receptors [10,17], and injection of GLP-1 or its analogs into brain tissue or ventricles produces effects on food intake, thermogenesis, and cardiovascular function [18–20]. Although it seems likely that PPG neurons are the source of GLP-1 released in the brain, the precise physiological role and cellular regulation of the activity of PPG neurons is still under intense discussion [21].

¹Centre for Cardiovascular and Metabolic Neuroscience, Department of Neuroscience, Physiology & Pharmacology, University College London, London, WC1E 6BT, UK ²Cardiovascular Medicine, Human Physiology and Centre for Neuroscience, Flinders University, Bedford Park, SA 5042, Australia ³Cambridge Institute for Medical Research, University of Cambridge, Addenbrooke's Hospital, Hills Road, Cambridge, CB2 0QQ, UK

*Corresponding author. Centre for Cardiovascular and Metabolic Neuroscience, Department of Neuroscience, Physiology and Pharmacology, University College London, London, WC1E 6BT, UK. E-mail: s.trapp@ucl.ac.uk (S. Trapp).

Abbreviations: 5-HT, 5-hydroxytryptamine; CCK-8, cholecystokinin-8; CNS, central nervous system; GLP-1, glucagon-like peptide-1; HPA, hypothalamic–pituitary–adrenal; IRT, intermediate reticular nucleus; NTS, nucleus tractus solitarius; PBN, parabrachial nucleus; PPG, preproglucagon; YFP, yellow fluorescent protein

Received April 27, 2017 • Revision received June 1, 2017 • Accepted June 5, 2017 • Available online 7 June 2017

<http://dx.doi.org/10.1016/j.molmet.2017.06.002>

Serotonin (5-hydroxytryptamine; 5-HT) is another key neurotransmitter involved in both regulation of stress and anxiety and control of food intake [22–24]. 5-HT serves complex roles centrally, reflected in a diverse range of 5-HT receptor subtypes and widespread distribution of 5-HT receptor-expressing neurons within the brain. Receptors are expressed postsynaptically on both dendrites and somata and pre-synaptically on synaptic terminals and can be either inhibitory or excitatory. A variety of 5-HT receptor subtypes have been implicated in the regulation of food intake, including 5-HT₃ [25], 5-HT_{2C} [26], 5-HT_{1A} [27], and 5-HT_{1B} [28]. To facilitate development of new obesity treatments, it is crucial to understand the underlying circuitry and the potential interactions with other anorexigenic and anxiogenic systems such as the brain GLP-1 system. 5-HT_{2C} receptors are important for control of food intake and loss-of-function mutation of the 5-HT_{2C} receptor leads to increased food intake, obesity and impaired glucoregulation [29,30]. Interestingly, the food intake-suppressing effect of GLP-1 administered intraperitoneally was abolished in a mouse lacking 5-HT_{2C} receptors, suggesting a link between GLP-1 and serotonergic regulation of food intake [31,32].

PPG neurons heavily innervate serotonergic neurons in the caudal raphe nuclei [33]; but it is currently unclear whether PPG neurons in turn receive serotonergic input. Patch-clamp electrophysiology demonstrated that PPG neurons are activated by the satiety hormones leptin and cholecystokinin-8 (CCK-8) as well as by glutamate and adrenaline [34,35]. Although patch-clamp electrophysiology provides a highly sensitive method of characterizing the electrical properties of individual neurons, it is limited to recording from single cells. In contrast, genetically encoded Ca²⁺ indicators allow for the monitoring of the activity of entire functionally distinct populations of neurons [36]. In this study, we have investigated the cellular effects of 5-HT on PPG neurons, as well as the innervation that underlies these effects. We found that 5-HT-immunoreactive axons closely apposed PPG cell bodies and dendrites in the NTS. Using transgenic mice expressing the GFP-based Ca²⁺ sensor GCaMP3 selectively in the PPG neurons [37], we characterized the responses to 5-HT of both PPG cell bodies and dendrites [38]. In addition, cell-attached patch-clamp recordings allowed us to determine how 5-HT affected the action potential firing patterns of PPG neurons. 5-HT modulated PPG neuronal activity with different outcomes in dendrites and somata. Dendritic activation by 5-HT was dependent on 5-HT₂ receptors and 5-HT_{2C} receptor activation was sufficient to elicit dendritic Ca²⁺ rises in PPG neurons. Interestingly, the Ca²⁺ changes in PPG neurons were compartmentalized with dendritic spikes failing to propagate to somata. In addition, about half of PPG neurons were found to decrease firing rate upon application of 5-HT, an effect that was abolished by blockade of 5-HT_{1A} receptors. These data suggest a multifaceted link between 5-HT and central GLP-1, which is tightly regulated through excitatory or inhibitory responses to 5-HT occurring within different subcellular compartments of PPG neurons.

2. MATERIALS AND METHODS

2.1. Transgenic animals

Two transgenic mouse strains were used in this study. The GLU-124 Venus YFP strain (YFP-PPG) [9,39], which expresses YFP in PPG cells, was used for the immunohistochemical experiments. Mice expressing GCaMP3 in PPG neurons were obtained by crossing transgenic mice expressing Cre recombinase under the control of the glucagon promoter (GLU-Cre12) [40] with a ROSA26-lox-stop-lox-GCaMP3 reporter mouse as described earlier (GCaMP3-PPG) [37]. Mice were bred as homozygotes and kept on a 12 h light: 12 h dark

cycle with *ad libitum* access to food and water. All experiments were carried out in accordance with the U.K. Animals (Scientific Procedures) Act, 1986, with appropriate ethical approval.

2.2. Immunohistochemistry

We used a total of three male and three female adult YFP-PPG mice. They were perfused at 12–16 weeks after birth and the tissue was processed as described earlier [33]. Both primary antibodies used here have been characterized previously in our laboratory [9,33] and exhibit specificity.

Briefly, the medullas of YFP-PPG mice were blocked without the use of a brain matrix, infiltrated with sucrose and cut into three series of transverse 30 μm cryostat sections. Sections were first washed 3 × 10 min in 10 mM Tris, 0.9% NaCl, 0.05% thimerosal in 10 mM phosphate buffer, pH 7.4, (TPBS) containing 0.3% Triton X-100, and then exposed to TPBS-Triton containing 10% normal horse serum (NHS) for at least 30 min. Diluents were TPBS-Triton containing 10% NHS for primary antibodies; TPBS-Triton containing 1% NHS, for secondary antibodies; and TPBS-Triton, for avidin-horseradish peroxidase. Immunohistochemistry was done at room temperature on a shaker and washes were in TPBS for 3 × 10 min after each exposure to an immunoreagent.

Antigens were localized with our standard avidin-biotin-peroxidase protocol and either black or brown diaminobenzidine (DAB) reaction products. Sections that had been washed in TPBS-Triton and exposed to 10% NHS as above were transferred into 1:5000 rabbit anti-5-HT (Catalog #8250-0009, Lot #23073052; Biogenesis, Poole UK) for 2–3 days. After washing, sections were incubated overnight in a biotinylated donkey anti-rabbit immunoglobulin (Ig; 1:500; Jackson ImmunoResearch, West Grove PA) followed by a 4–6 h incubation in ExtrAvidin-peroxidase (1:1500; Sigma–Aldrich, St Louis MO, USA). A cobalt + nickel-intensified DAB reaction using peroxide generated by glucose oxidase [41] stained structures immunoreactive for 5-HT black. After 5-HT had been localized, the sections were washed and underwent another blocking step in NHS. Then the immunohistochemical protocol above was repeated to localize YFP with 1:50,000 chicken anti-GFP (Catalog #ab13970, Lot #623923; Abcam, Cambridge, UK). YFP-immunoreactive structures were stained brown with an imidazole-intensified DAB reaction in which peroxide production was catalyzed by glucose oxidase [41].

We examined stained sections from the spinomedullary junction to the rostral end of the area postrema with an Olympus BH-2 brightfield microscope equipped with a SPOT color camera (Diagnostic Instruments Inc., Sterling Heights, MI, USA). Images were captured as TIFF files using SPOT software v5.2 and exported to Adobe PhotoShop for adjustment of sharpness, brightness, and contrast. Montages of micrographs and plates were prepared with PhotoShop. Using an ×100 oil immersion lens, we quantified close appositions from 5-HT-immunoreactive axon terminals onto YFP-immunoreactive cell bodies and dendrites in one female and two male mice.

GCaMP3 immunoreactivity was detected with an antibody raised against green fluorescent protein (GFP; Catalog #AB13970, lot #623923; Abcam, Cambridge, UK) as previously described [37]. Briefly, 30 μm cryostat sections were blocked with 0.1% Triton X-100 and 10% normal goat serum diluted in 0.1 M phosphate buffer (PB), pH 7.4, for 1 h at room temperature. The primary antibody was added to the blocking solution at a 1:1000 dilution and incubated overnight at 4 °C. Subsequently, sections were washed 5 × 5 min in 0.1 M PB at room temperature, followed by incubation with Alexa Fluor 488-conjugated goat anti-chicken antibody (1:500; Catalogue# A-11039, Invitrogen) in blocking solution for 2 h.

2.3. Ca²⁺ imaging and electrophysiology

On the morning of imaging, GCaMP3-PPG mice were deeply anesthetized using isoflurane and decapitated. The brainstem was removed and placed in ice-cold high-Mg²⁺/low-Ca²⁺ artificial cerebrospinal fluid (ACSF; composition in mM: 2.5 KCl, 200 sucrose, 28 NaHCO₃, 1.25 NaH₂PO₄, 7 Glucose, 7 MgCl₂, 0.5 CaCl₂; pH 7.4). We cut 200 μm-thick coronal brainstem slices on a vibratome (7000smz2, Campden Instruments) and incubated them in recovery solution (in mM: 3 KCl, 118 NaCl, 25 NaHCO₃, 1.2 NaH₂PO₄, 2.5 Glucose, 7 MgCl₂, 0.5 CaCl₂; pH 7.4) at 34 °C for 45 min. Sections were then transferred to standard ACSF (in mM: 3 KCl, 118 NaCl, 25 NaHCO₃, 10 Glucose, 1 MgCl₂, 2 CaCl₂; pH 7.4) and left at 34 °C for a minimum of 30 min before imaging. All solutions were constantly bubbled with 95% O₂/5% CO₂.

Electrophysiological recordings in the cell-attached configuration were performed as described previously [42] and analyzed with Strathclyde Electrophysiology Software (WinEDR/WinWCP; University of Strathclyde, Glasgow, United Kingdom). The response firing rate was defined as the average firing rate over 1 min when the firing rate was at its most extreme during the stimulus. Responding cells were identified by determining whether the response firing rate was significantly different to baseline firing rate over 1 min prior to the 5-HT stimulus using Student's T-test. $p < 0.05$ was taken as statistically significant.

All imaging was performed on PPG neurons in the NTS. Ca²⁺ imaging was performed in one of two configurations: 1) with a Zeiss Axioskop 2FS widefield microscope using a 40× water immersion lens. GCaMP3 was excited using an LED light source (CoolLED pE300white; QImaging) at 460 nm (± 25 nm) for 250 ms every 5 s. Images were captured at 12-bit on a charge-coupled device camera (Q-Click; QImaging). 2) with an Olympus FV-1000 scanning confocal microscope using a 25× water immersion lens. GCaMP3 was excited using a laser at 488 nm; emission was recorded at 520 ± 10 nm. Emitted light was detected using a photon-multiplier tube. We observed no difference in the response to 5-HT between the two systems, though bleaching and background fluorescence had to be corrected for only when using the widefield microscope. Slices were continuously superfused with 32 °C standard ACSF at a flow rate of 3–4 ml/min. All drugs were added directly to ACSF. Serotonin hydrochloride (5-HT; 2, 20 and 200 μM), WAY161,503 hydrochloride (5 μM) and TTX-citrate (0.5 μM) were purchased from Tocris Bioscience. 6,7-Dinitroquinoxaline-2,3(1H,4H)-dione (DNQX; 20 μM), 1-Phenylbiguanide (PBG; 1 and 10 μM), granisetron (5 μM), ketanserin (1 μM) and WAY100,635 maleate salt (20 μM) were obtained from Sigma. For recordings in 0 mM Ca²⁺, 2 mM CaCl₂ was replaced with 2 mM MgCl₂. Data was collected from at least three different experiments, using tissue derived from at least three mice, for each condition.

2.4. Analysis of Ca²⁺ imaging data

Recordings were imported into FIJI image analysis software [43]. XY-drift was adjusted for using the StackReg plugin [44]. Regions of interest (ROIs) and an area for determining background fluorescent intensity were outlined and the mean pixel intensity calculated for each ROI. For time-lapse data recorded on the widefield microscope, background intensity was subtracted from each ROI and recordings were adjusted for bleaching using a cubic polynomial function [45]. Fluorescence intensity data are presented as $\Delta F/F_0$ with F_0 being the average fluorescence intensity 5 min prior to the first stimulus and ΔF being the fluorescence intensity, F , minus F_0 . N numbers indicate number of analyzed dendrites. Responses were quantified by calculating areas under the curve (AUC) over 10 min during the stimulus, starting at the beginning of the stimulus. Because they were found not to be normally distributed, summary data are presented as box plots

with whiskers, with the median indicated and whiskers marking the 10th and 90th percentile, respectively. Statistical significance was determined using nonparametric statistical testing; Friedman, Kruskal–Wallis or Wilcoxon as indicated in figure legends.

3. RESULTS

3.1. Serotonergic innervation of PPG neurons

5-HT-immunoreactive innervation of brainstem PPG neurons was assessed in three adult male and three adult female YFP-PPG mice. After peroxidase staining, PPG neurons in the NTS, the IRT and the midline ventral to the hypoglossal nucleus showed intense YFP staining throughout cell bodies and dendrites. The distribution of YFP-expressing neurons in the medulla of YFP-PPG mice was the same as reported before [9,33], with NTS PPG neurons forming the largest subpopulation and the midline neurons being the smallest.

5-HT-immunoreactive axons occurred throughout the caudal NTS and many PPG neurons in the NTS received close appositions from 5-HT axons on their somata and/or proximal dendrites (Figure 1A–D). In the NTS, 5-HT axons apposed 208 of 358 PPG neurons ($n = 3$ mice); the percentage of PPG neurons innervated by 5-HT axons in each mouse varied between 50% and 80%. In each rostro-caudal section analyzed, 5-HT appositions were preferentially targeted toward more medial PPG neurons whereas more lateral neurons usually lacked appositions (Figure 2).

The extent of 5-HT innervation of PPG neurons in the IRT was similar (Figure 1E), with 46% (67 of 147; $n = 3$ mice) of PPG neurons receiving close appositions. Innervation of midline PPG neurons was very sparse at 4% (2 of 46 PPG neurons with appositions; $n = 3$ mice).

3.2. Intracellular Ca²⁺ can be monitored using GCaMP3

To investigate the potential functional significance of these 5-HT appositions, we recorded intracellular Ca²⁺ changes in NTS PPG neurons in response to 5-HT. Transgenic mice selectively expressing the genetically encoded Ca²⁺ indicator GCaMP3 in PPG neurons (Figure 3A,B) were used to monitor changes in intracellular Ca²⁺ as a surrogate marker for neuronal activity. GCaMP3 was detected in the caudal part of the NTS (Figure 3B) and in the dorsomedial part of the intermedial reticular nucleus (data not shown). GCaMP3-expressing neurons have been shown previously to express GLP-1 in this transgenic mouse model [37]. To demonstrate the ability to record changes in intracellular Ca²⁺ from PPG neurons *in vitro*, coronal brainstem slices were superfused with 100 μM glutamate for 1 min. Intracellular Ca²⁺ rapidly increased in 89% of imaged cell bodies as well as proximal dendrites in response to 100 μM glutamate and returned to baseline after washout of the drug (Figure 3D), demonstrating that rises in intracellular Ca²⁺ are detectable. We have previously shown using patch-clamp electrophysiology that the satiety hormones, leptin and CCK-8, activate PPG neurons in the NTS [34,35]. Now, using Ca²⁺ imaging, we confirm those findings (Figure 3C). 1 nM leptin increased intracellular Ca²⁺ in all imaged PPG neurons ($n = 17$ cells), whereas only a subset of NTS PPG neurons exhibited activation upon superfusion with 200 nM CCK-8 (five out of 14 imaged PPG neurons). These data along with previously published immunohistochemical verification [37] validate our model and demonstrate that it is well-suited to investigate responses to other neurotransmitters.

3.3. PPG distal dendrites are activated by 5-HT

We next investigated the response of PPG neurons to 5-HT. PPG neurons were exposed to 20 μM 5-HT for 1 min. In the recording shown in Figure 3E, only one cell body responded to 20 μM 5-HT with an increase in intracellular Ca²⁺ (blue trace), although all cell bodies

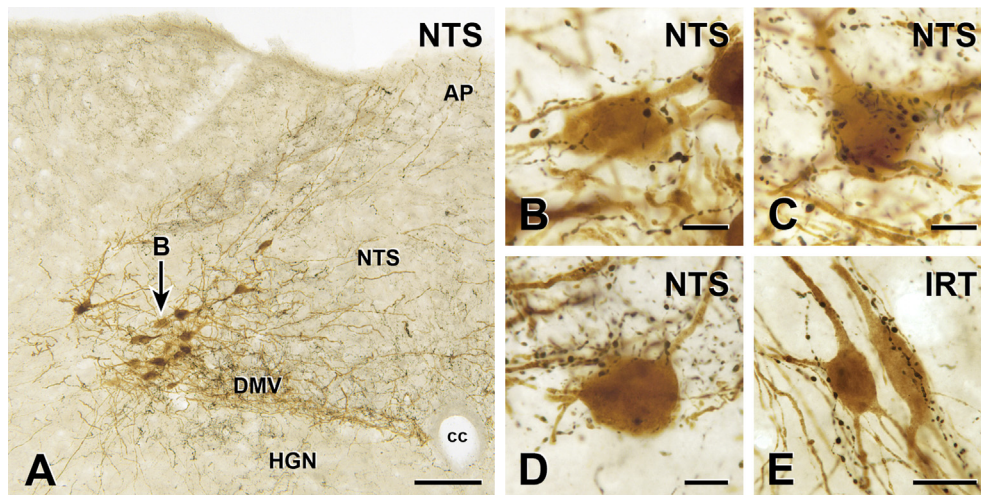


Figure 1: PPG neurons receive close appositions from 5-HT immunoreactive axons. Two-color immunoperoxidase labeling for YFP-immunoreactivity in YFP-PPG neurons (brown) and 5-HT-immunoreactivity in serotonergic neurons (black) in transverse sections through the dorsal vagal complex (DVC) of YFP-PPG mice. (A) Montage of low magnification micrographs showing YFP-immunoreactive PPG cell bodies (brown) and 5-HT-immunoreactive axons (black) in the DVC. The cell body indicated by the arrow is shown at higher magnification in B. Scale bar = 100 μm . (B, C, D) Brown YFP-immunoreactive cells bodies and dendrites in the NTS receive close appositions from black 5-HT-immunoreactive axons. Scale bars = 10 μm . (E) A YFP-immunoreactive cell body in the IRT receives close appositions from 5-HT-immunoreactive axons. Scale bar = 20 μm . AP: area postrema; cc: central canal; DMV: dorsal motor nucleus of the vagus; HGN: hypoglossal nucleus; NTS: nucleus tractus solitarius.

responded to 100 μM glutamate ($n = 8$ somata). In total, only four out of 39 imaged cell bodies increased intracellular Ca^{2+} in response to 20 μM 5-HT. However, dendrites adjacent to PPG cell bodies responded with rapid, transient rises in intracellular Ca^{2+} (Figure 3F, $n = 19$ dendrites). The dendritic response was found to be concentration-dependent; 2 μM 5-HT increased dendritic Ca^{2+} spikes to a lesser degree than either 20 μM or 200 μM (Figure 3F right panel, Friedman test, $p < 0.0001$, $n = 88$ dendrites (4 mice)). Although cells were only exposed to 5-HT for 1 min, dendritic activity persisted after washout of 5-HT (Figure 3F) and lasted for 3.5 ± 0.2 min.

3.4. PPG neurons have functional 5-HT₂ receptors

To investigate the source of Ca^{2+} for these responses, we applied 20 μM 5-HT in the absence of extracellular Ca^{2+} . Removal of extracellular Ca^{2+} reduced the response to 20 μM 5-HT by $69 \pm 12\%$ (Figure 4A, $n = 28$ (3 mice)). We next asked whether the responses of PPG neurons to 5-HT are dependent on the activity of neighboring cells. By blocking voltage-gated sodium channels with TTX and glutamatergic input with the AMPA/kainate receptor antagonist DNQX, we synaptically isolated the PPG neurons. This assumption is based on our previous observation that blockade of ionotropic non-NMDA receptors inhibits $>90\%$ of spontaneous EPSCs in PPG neurons [34,35]. The response to 5-HT was unaffected by TTX and DNQX, suggesting that PPG neurons have functional 5-HT receptors (Figure 4B, $n = 55$ dendrites (4 mice)).

Most 5-HT receptor subtypes are expressed in the NTS [46,47]. 5-HT₂ and 5-HT₃ receptor activation is associated with a reduction in food intake; consequently, we assessed the potential contribution of either of these receptors to the response to 5-HT in PPG neurons. The 5-HT₃ receptor agonist phenylbiguanide (PBG) failed to elicit Ca^{2+} changes at two different concentrations (Figure 5A; 1 μM PBG, $n = 22$ dendrites and 10 μM PBG, $n = 25$ dendrites; 20 μM 5-HT, $n = 37$ dendrites (3 mice)) and 5 μM granisetron, a 5-HT₃ receptor antagonist, was unable to block the response to 20 μM 5-HT (Figure 5B, $n = 32$ dendrites (3 mice), $p = 0.12$). These findings suggest that 5-HT₃ receptors are not involved in the response of PPG neurons to 5-HT. In contrast, blocking

5-HT₂ receptors with 1 μM ketanserin attenuated the response to 5-HT by $77 \pm 6\%$ (Figure 5C, $n = 17$ dendrites (3 mice)).

Next we tested whether the 5-HT_{2C} receptor agonist WAY161,503 is able to elicit dendritic Ca^{2+} spikes in PPG neurons because 5-HT_{2C} receptors are well known to be involved in the regulation of food intake. WAY161,503 (5 μM) elicited transient rises in Ca^{2+} in PPG dendrites in a total of five different sections from five different animals (Figure 5D, $n = 32$ dendrites (5 mice)). This response to 5-HT_{2C} receptor activation suggests that 5-HT activates PPG neuronal dendrites via 5-HT_{2C} receptors.

3.5. 5-HT modulates spontaneous firing activity of PPG neurons

The results above demonstrate that PPG neurons receive 5-HT synaptic inputs and that activation of 5-HT_{2C} receptors modulates intracellular Ca^{2+} concentration in PPG dendrites *in vitro*. Next, we explored whether these dendritic changes in intracellular Ca^{2+} reflect a change in the electrical output from these cells. We used extracellular recordings in the loose-patch configuration to monitor the pattern of spontaneous action potential discharges in PPG neurons without breaking the cell membrane and diluting cytosolic proteins. This approach enabled us to record electrical activity and cytosolic Ca^{2+} simultaneously, because GCaMP3 was not diluted into the patch-pipette. Of the 16 cells recorded, seven reduced their firing rate in the presence of 20 μM 5-HT (Figure 6B); four cells showed no response and five increased their firing rate (Figure 6A,C). A significant reduction in firing rate was accompanied by a small, but clear reduction in intracellular Ca^{2+} concentration (Figure 6D), demonstrating that ongoing electrical activity strongly affects the intracellular Ca^{2+} concentration in PPG neurons. This correlation between firing rate and intracellular Ca^{2+} concentration is further demonstrated in Figure 6D, right panel.

Having established that 5-HT reduces firing rate in a proportion of PPG neurons, we next addressed the question which 5-HT receptors are involved in this response. Only 5-HT₁ and 5-HT₅ receptors couple to the $G_{i/o}$ pathway [48] and 5-HT_{1A} receptor inhibition reduces food intake [27]. We therefore tested in four PPG neurons that decreased

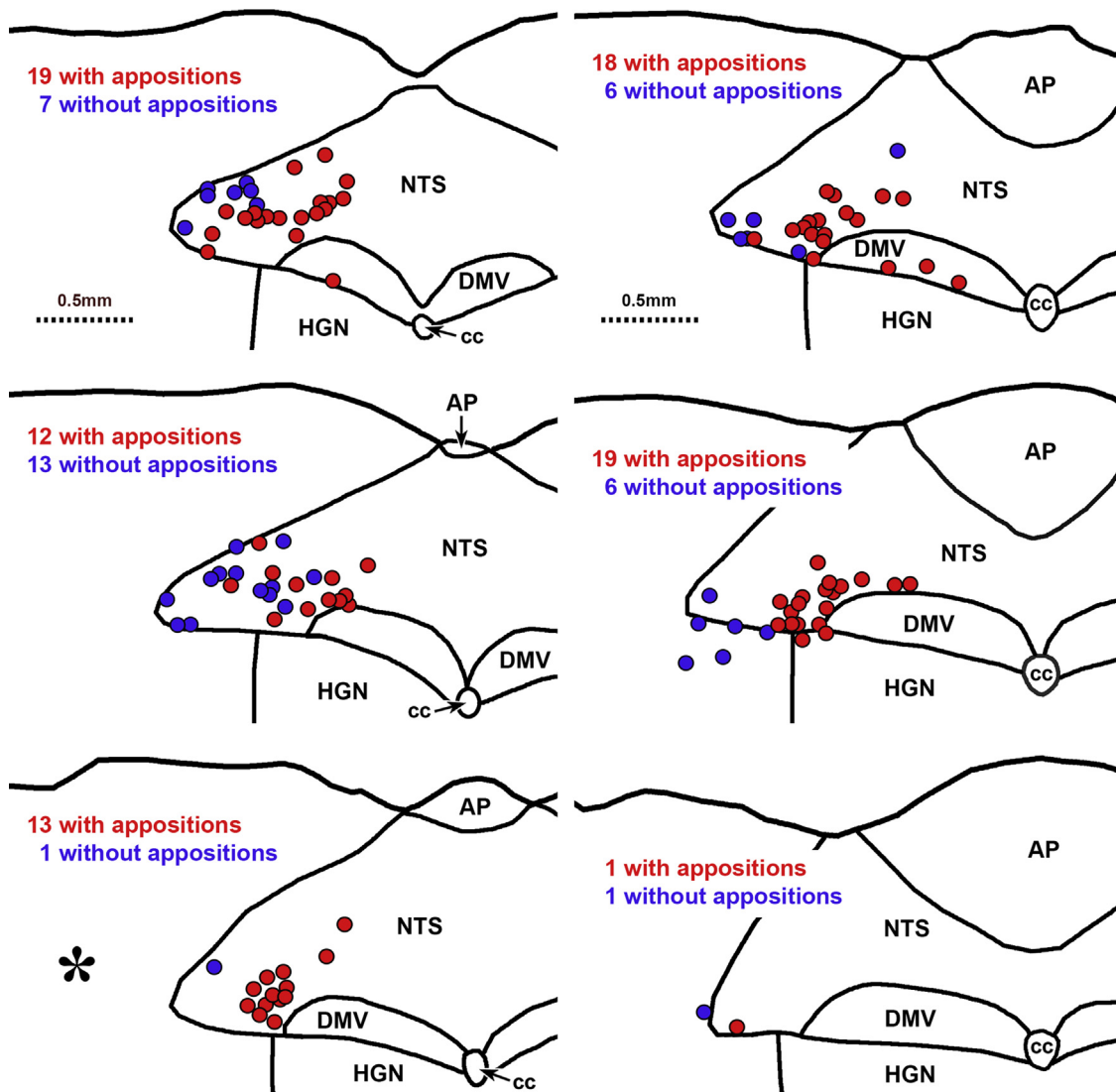


Figure 2: Maps of sections through the dorsal vagal complex of a YFP-PPG mouse showing the distribution of YFP-immunoreactive neurons with and without close appositions from 5-HT-immunoreactive varicosities. Every third section through the brainstem was stained to reveal YFP and 5-HT and then mapped; maps are therefore separated by 60 μm . The most caudal section is at the top left of the figure and the most rostral section is at the bottom right. YFP-immunoreactive neurons are represented by circles. Neurons that receive close appositions from 5-HT-immunoreactive varicosities are shown in red; those that do not receive appositions are shown in blue. [Figure 1A](#) shows the section with the asterisk. NTS, nucleus tractus solitarius; AP, area postrema; DMV, dorsal motor nucleus of the vagus; HGN, hypoglossal nucleus; cc, central canal.

firing rate under 5-HT whether the selective 5-HT_{1A} receptor antagonist WAY-100,635 reduces the inhibitory effect, and whether 5-HT_{1A} receptor inhibition facilitates somatic Ca²⁺ rises under 5-HT by blocking inhibitory responses. [Figure 7A](#) shows a representative loose-patch recording from a PPG neuron that was strongly inhibited by 5-HT (left) along with the change in fluorescence intensity of the same cell (top left; red trace). Action potential firing ceased almost completely upon application of 20 μM 5-HT. In the presence of WAY100,635, the inhibitory response to 5-HT was prevented as documented in both the Ca²⁺ imaging trace and the firing frequency but did not turn into a 5-HT-mediated excitation in any of the four cells tested (bottom right). Somatic Ca²⁺ recordings produced a similar result with seven cells that showed a clear reduction in intracellular Ca²⁺, losing that inhibitory response in the presence of WAY100,635 ([Figure 7A](#) top right). Interestingly, the dendritic response to 20 μM 5-HT was not altered in the presence of WAY100,635 ([Figure 7B](#): left panel, n = 6; right panel, 5-HT, n = 248; right panel, +WAY100,635, n = 20 (3 mice)),

demonstrating that blocking inhibitory 5-HT receptors does not increase excitation.

4. DISCUSSION

In this study, we explored potential anatomical and functional links between 5-HT and GLP-1 neurons within the brainstem. First, we demonstrated that GLP-1-producing PPG neurons in the medulla receive close appositions from 5-HT-immunoreactive axons. We found close appositions from serotonergic axons on the somata or proximal dendrites of 58% of PPG neurons in the NTS and lower levels of innervation of the PPG neurons in the IRT. Interestingly, midline PPG neurons received very sparse 5-HT input, suggesting these neurons could play a different physiological role to the NTS and IRT populations.

Despite almost two thirds of NTS PPG neurons receiving somatic or proximal dendritic close appositions, only 10% of these cells exhibited a

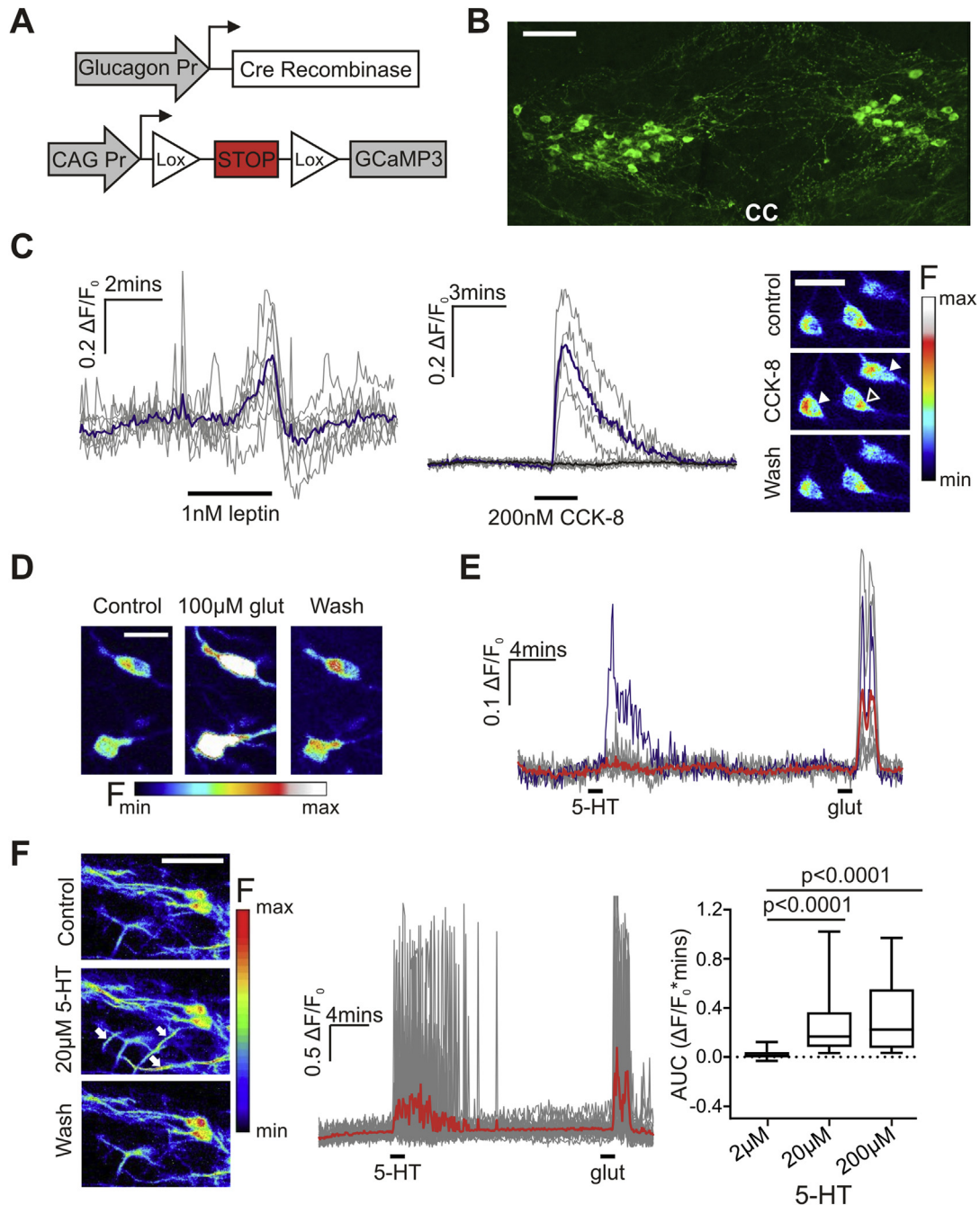


Figure 3: 5-HT evoked Ca^{2+} transients in PPG neurons are mainly observed in dendrites. (A) Intracellular Ca^{2+} changes in PPG neurons can be monitored using the genetically encoded Ca^{2+} indicator, GCaMP3. Glucagon promoter (Glu)-Cre mice were crossed with mice expressing CAG-promoter-STOP-GCaMP3 in the Rosa26 locus. The Rosa26 locus is active in most cell types. In cells with active glucagon promoter, the bacterial recombinase Cre is produced and excises the STOP sequence flanked by lox sites upstream of the GCaMP3 gene. This process results in cytosolic expression of GCaMP3 in these cells, detected here with an anti-GFP antibody (B; scale bar: 100 μm). (C) PPG neurons respond to both leptin (1 nM, n = 8 somata, left panel) and CCK-8 (200 nM, n = 12 somata, middle panel) with an increase in cytosolic Ca^{2+} . The panel on the right shows three pseudocolored cells, two of which (white arrowheads) show increased fluorescence intensity after application of 200 nM CCK-8. The black arrowhead indicates one cell that did not increase $[\text{Ca}^{2+}]_i$ in the presence of 200 nM CCK-8 (Scale bar: 30 μm). (D) GCaMP3 fluorescence intensity is sensitive to changes in cytosolic Ca^{2+} concentration. For example, bath application of 100 μM glutamate (glut) leads to a strong reversible rise in somatic Ca^{2+} concentration (Scale bar: 20 μm). The panel on the left shows two pseudocolored PPG neurons before, during and after stimulation with 100 μM glutamate. (E) Fluorescence intensity expressed as a fraction of the intensity at the beginning of the experiment. Traces from individual cells are plotted in gray or dark blue, and the average response is shown in red. While virtually every cell responded to 100 μM glutamate with a somatic Ca^{2+} transient, in this example, only one of nine PPG neurons responded to 20 μM 5-HT (shown in the dark blue trace). (F) Representative images showing dendritic GCaMP3 fluorescence intensity before, during and after 20 μM 5-HT. Arrows point to dendrites with transient increases in Ca^{2+} (Scale bar = 50 μm). Transient changes in intracellular Ca^{2+} in PPG dendrites (n = 19) in response to 20 μM 5-HT and 100 μM glutamate are shown in the middle. Measurements from individual regions of interest are shown in gray, the mean trace is shown in red. On the right, quantification of responses showing median AUC during the response to 2 μM , 20 μM , or 200 μM 5-HT (n = 88 dendrites (4 mice)). Friedman test (Chi-square = 60.03, p < 0.0001) followed by post-hoc comparisons revealed the response to 2 μM 5-HT to be significantly different to both 20 μM and 200 μM 5-HT (p < 0.0001 for both).

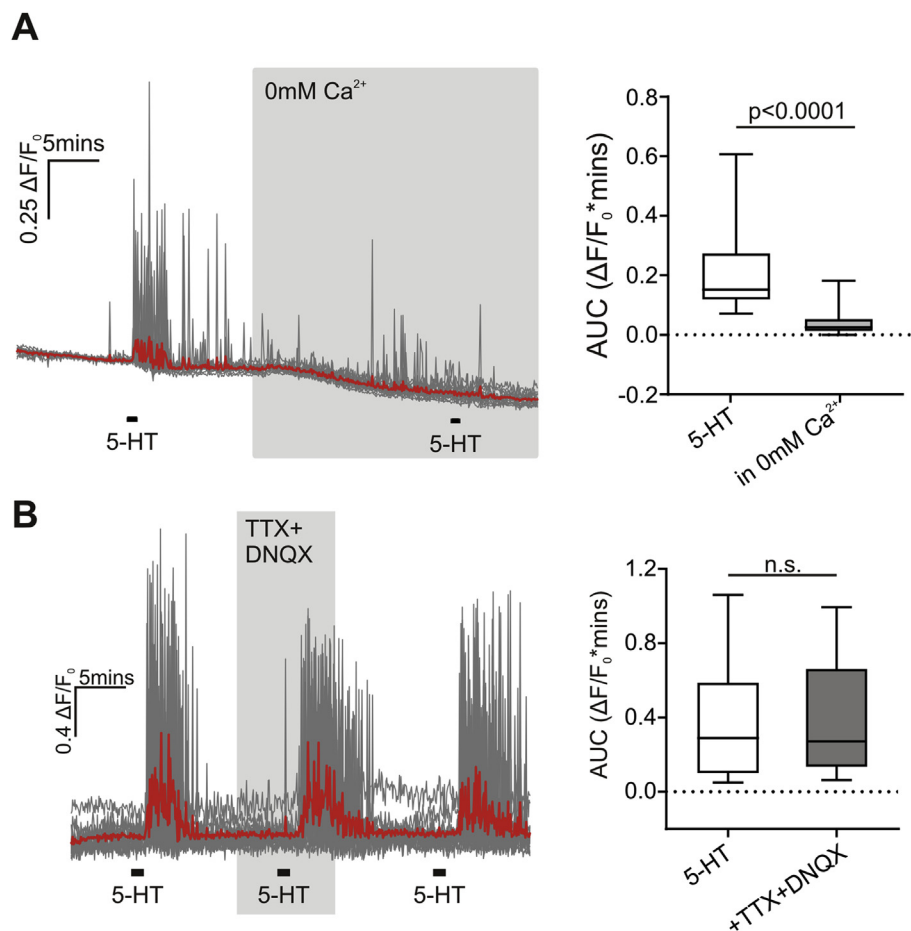


Figure 4: 5-HT activates PPG fibers directly and this is dependent on influx of extracellular Ca^{2+} . (A) Removal of extracellular Ca^{2+} attenuates the response to $20\ \mu\text{M}$ 5-HT. *Left panel:* Traces showing changes in intracellular Ca^{2+} with individual fibers shown in gray and the average trace in red ($n = 16$ dendrites). *Right panel:* Median AUC in response to $20\ \mu\text{M}$ 5-HT in the presence and absence of extracellular Ca^{2+} ($n = 28$ dendrites (3 mice); Wilcoxon test: $p < 0.0001$). (B) *Left panel:* Traces showing the response to $20\ \mu\text{M}$ 5-HT in the presence or absence of TTX ($0.5\ \mu\text{M}$) and DNQX ($20\ \mu\text{M}$) ($n = 8$ dendrites). *Right panel:* Median AUC during the response to $20\ \mu\text{M}$ 5-HT in the absence (white box) or presence (gray box) of TTX and DNQX ($n = 55$ dendrites (4 mice)). Wilcoxon test: $p = 0.56$ n.s.: not significant.

somatic rise in intracellular Ca^{2+} upon exposure to 5-HT and approximately a quarter of PPG neurons increased their electrical activity in response to 5-HT. However, we also observed that 5-HT application reduced electrical activity in almost 50% of the NTS PPG neurons tested. This finding suggests that most of the axosomatic close appositions from 5-HT terminals onto PPG neurons reflect inhibitory inputs. The majority of Ca^{2+} increases in response to 5-HT were recorded in dendrites with little observable propagation of the Ca^{2+} signal to cell bodies. We were therefore unable to quantify the percentage of PPG neurons that were excited by 5-HT at dendritic level. We found that dendritic Ca^{2+} rises evoked by 5-HT persisted in the presence of TTX and DNQX. These observations support the notion that the dendritic responses are due to activation of postsynaptic 5-HT receptors rather than presynaptic receptors that increase glutamate release onto PPG neurons, as we observed for CCK [34] and as was reported for 5-HT on A2 catecholaminergic NTS neurons [49].

4.1. Excitatory 5-HT responses

5-HT₃ receptors are strongly expressed on vagal afferent terminals in the NTS, and we have previously demonstrated that PPG neurons receive both mono- and polysynaptic inputs from vagal afferents [35]. Interestingly, however, neither selective activation of 5-HT₃ receptors nor selective inhibition of these receptors during 5-HT application

significantly changed Ca^{2+} concentrations in PPG neurons. This result argues that PPG neurons do not express 5-HT₃ receptors and suggests that vagal afferents expressing 5-HT₃ receptors do not impinge upon these cells. However, it should be noted that we cannot categorically exclude that a 5-HT-induced increase in glutamatergic postsynaptic potentials from vagal afferents may fail to affect intracellular Ca^{2+} in PPG neurons sufficiently to be detected using GCaMP3. Nevertheless, activation of any presynaptic 5-HT₃ receptors should have measurably affected Ca^{2+} concentrations in PPG neurons since our combined loose-patch recordings and our Ca^{2+} recordings showed a close correlation between Ca^{2+} levels and electrical activity. Our finding that PPG neurons do not express 5-HT₃ receptors is consistent with the observation by Appleyard and colleagues that, while the vast majority of A2/C2 neurons in the NTS respond to 5-HT₃ receptor activation, only a small fraction of non-catecholaminergic cells do [49]. 5-HT released from serotonergic axons in the NTS acts on 5-HT₃ receptors to provide a strong anorexic drive to the parabrachial nucleus (PBN) [50]. Because our results demonstrate that PPG neurons do not have functional 5-HT₃ receptors, we conclude that PPG neurons do not directly contribute to the NTS – PBN projection underlying this hypophagic drive.

The 5-HT input to PPG neurons identified here seems to act on 5-HT₂ rather than 5-HT₃ receptors. 5-HT_{2C} receptors have been implicated in

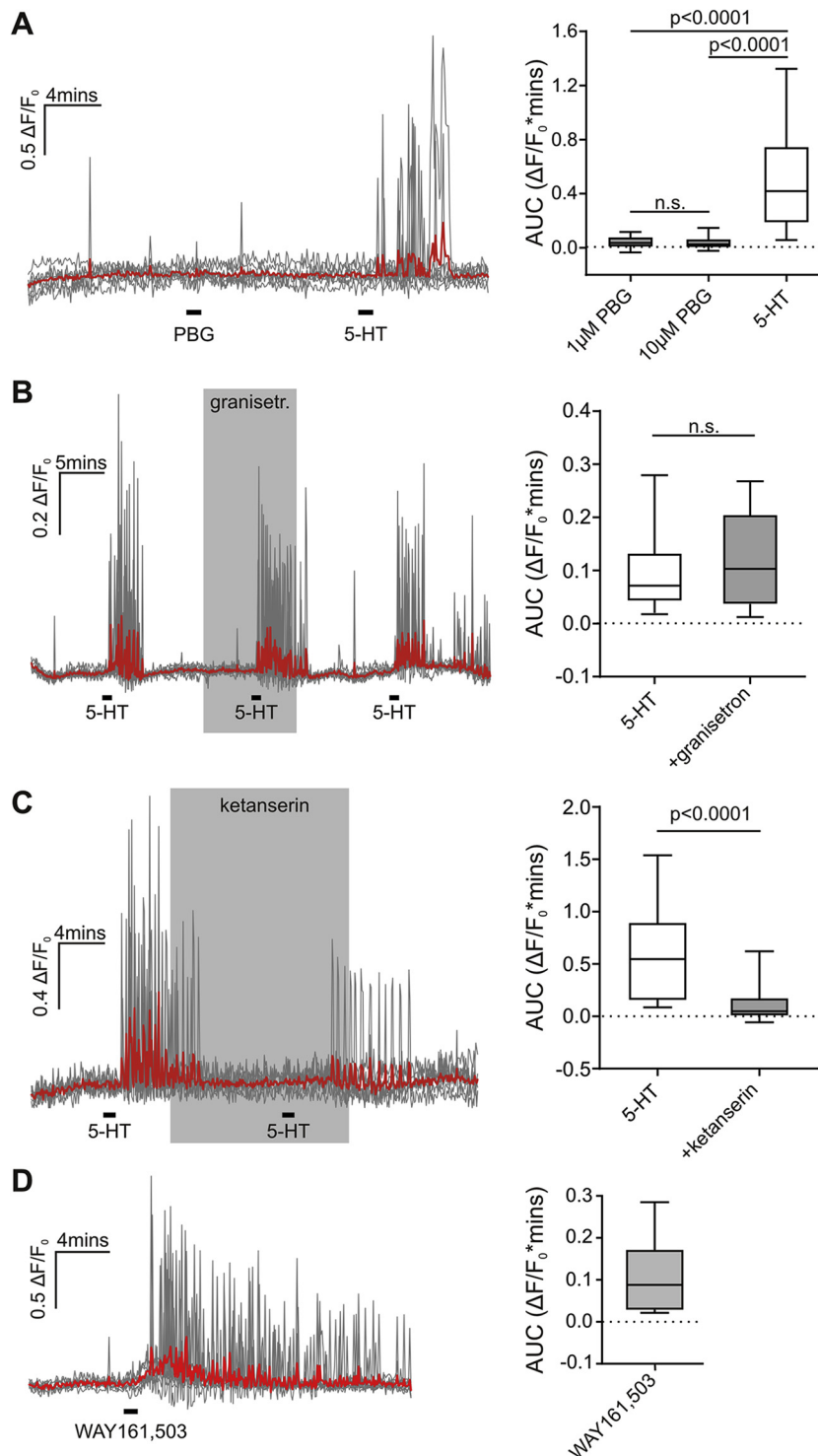


Figure 5: PPG neurons are activated by 5-HT via 5-HT₂ but not 5-HT₃ receptors and respond to 5-HT_{2C} receptor activation with an increase in dendritic Ca²⁺. (A) *Left panel:* Traces showing the responses to 20 μM 5-HT or 10 μM PBG (n = 7 dendrites), with individual fibers shown in gray and the average trace in red. *Right panel:* Median AUC during the response to 20 μM 5-HT (n = 37 dendrites), 1 μM PBG (n = 32 dendrites) or 10 μM PBG (n = 25 dendrites) (3 mice). Kruskal–Wallis rendered a Chi-Square value of 45.9 ($p < 0.0001$). Post-hoc comparisons revealed no statistically significant difference between 1 μM and 10 μM PBG ($p > 0.999$) but showed that the responses to 20 μM 5-HT were significantly different to both 1 μM and 10 μM PBG ($p < 0.0001$). (B) *Left panel:* Traces showing the response to 20 μM 5-HT in the absence and presence of 5 μM granisetron (granisetron; n = 6 dendrites). Individual fibers are shown in gray and the average trace in red. *Right panel:* Median AUC for the response to 20 μM 5-HT before (white box) and during (gray box) 5 μM granisetron (n = 32 dendrites) (3 mice). Wilcoxon test: $p = 0.12$. (C) *Left panel:* Representative traces showing the response to 20 μM 5-HT in the absence and presence of 1 μM ketanserin (n = 6 dendrites). *Right panel:* Median AUC for the response to 20 μM 5-HT in the absence (white box) or presence (gray box) of 1 μM ketanserin (n = 17 dendrites) (3 mice). Wilcoxon test: $p < 0.0001$. (D) *Left panel:* Representative traces showing the response to 5 μM WAY161,503, a 5-HT_{2C} receptor agonist (n = 9 dendrites). *Right panel:* Median AUC for the response to 1 min 5 μM WAY161,503 (n = 32 dendrites) (5 mice). n.s.: not significant.

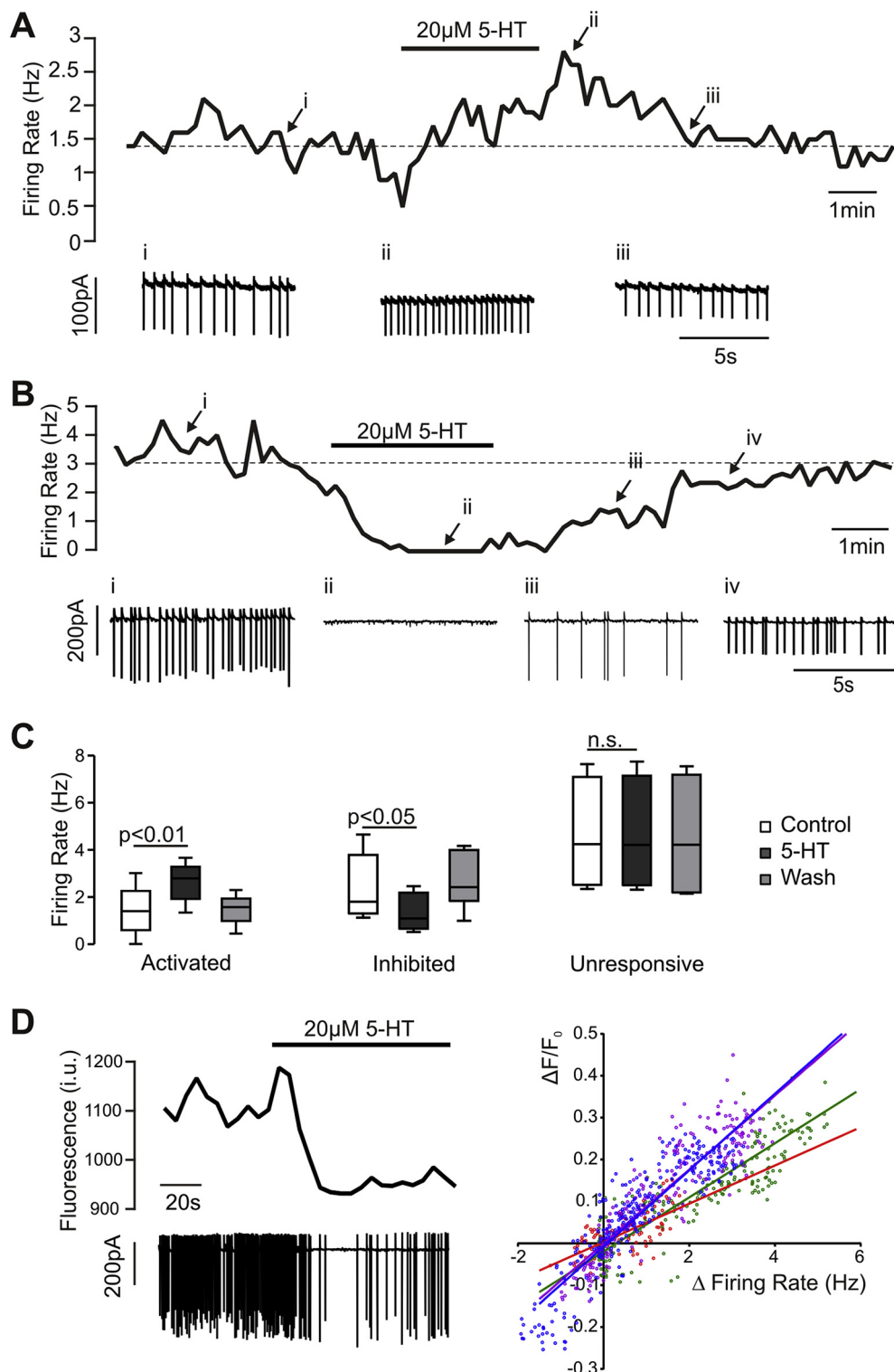


Figure 6: 5-HT modulates the electrical activity of PPG neurons. (A,B) Spontaneous firing rate recorded from PPG neurons in loose-patch cell-attached configuration. Periods of the original recordings at time points i, ii, iii, and iv are displayed below the graphs of instantaneous firing rate. Some PPG neurons are activated by 5-HT (A), whereas others are inhibited (B) or do not change their firing rate (not shown). (C) Box and whiskers plot of data from cells that were activated ($n = 5$ cells) or inhibited ($n = 7$ cells) by 5-HT and from cells that did not change their firing rate in response to 5-HT ($n = 4$) (data from 8 mice). A one-way within subjects ANOVA revealed a significant effect of 5-HT in the activated ($p < 0.01$) and inhibited ($p < 0.01$) cells but not in the unresponsive cells. A post-hoc analysis (Tukey) revealed a statistically significant increase in firing rate compared to baseline in the activated cells ($p < 0.01$) and a decrease in the inhibited cells ($p < 0.05$). (D) *Left panel:* Simultaneous recording of firing activity in attached patch configuration (bottom trace) and of intracellular Ca^{2+} (top trace, i.u.: intensity units) revealed a positive correlation between firing rate and intracellular Ca^{2+} concentration. The black bar indicates application of 20 μ M 5-HT. *Right panel:* Correlation between changes in firing rate and intracellular Ca^{2+} levels for four individual cells analyzed. Each cell is represented by a unique color, individual data points are represented by dots and a linear fit to the data is plotted in the same color (data from 3 mice).

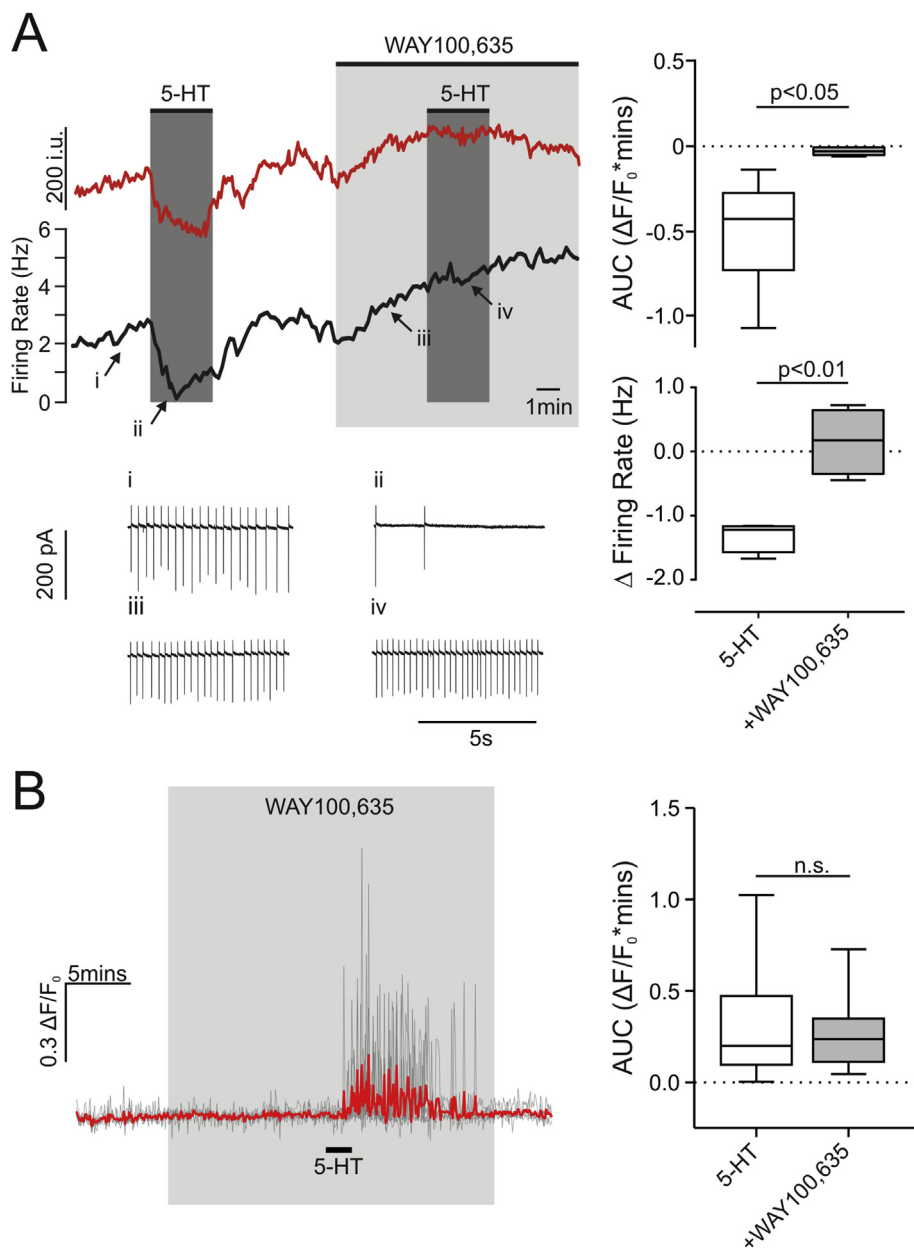


Figure 7: 5-HT inhibition of PPG neuron firing rate is dependent on 5-HT_{1A} receptors. (A) Change in GCaMP3 fluorescence (top left panel, i.u.: intensity units) and spontaneous firing rate (middle panel) from a PPG neuron recorded in the loose-patch cell-attached configuration. Applications of 20 μ M 5-HT are indicated by dark gray boxes and application of 5-HT_{1A} receptor antagonist, WAY100,635 (20 μ M), by a light gray box. Raw recordings at time points i, ii, iii, iv are shown in the bottom left panel. *Bottom right panel:* Summary data comparing the change in firing rate in response to 5-HT alone and in the presence of WAY100,635 ($n = 4$ cells (4 mice)). Paired Student's *t*-test: $p < 0.01$. *Top right panel:* Ca^{2+} recordings from seven somata. Intracellular Ca^{2+} decreased in response to 5-HT. This inhibitory effect of 5-HT was absent in the presence of WAY100,635 ($n = 7$ somata (3 mice)). Wilcoxon test: $p < 0.05$. (B) *Left panel:* The dendritic response to 5-HT was unchanged in the presence of 20 μ M WAY100,635 ($n = 6$ dendrites). The black bar indicates application of 20 μ M 5-HT. The light gray box indicates WAY100,635 application. *Right panel:* Summary data comparing 5-HT alone from previous experiments ($n = 248$ dendrites) with 5-HT in the presence of WAY100,635 ($n = 20$ dendrites (3 mice)). n.s.: not significant ($p = 0.91$) according to Mann–Whitney test.

the control of food intake via the melanocortin system in the hypothalamus [51]. We show here that 5-HT-induced dendritic Ca^{2+} spikes are dependent on 5-HT₂ receptors and that activation of 5-HT_{2C} receptors increases dendritic Ca^{2+} in NTS PPG neurons. Whether activation of 5-HT_{2C} receptors on PPG neurons contributes to the anorexic effects of, for example, the 5-HT_{2C} receptor agonist lorcaserin remains to be determined. Whilst the anorexic 5-HT receptor agonist m-chlorophenylpiperazine (mCPP) failed to elicit Fos-immunoreactivity in rat PPG neurons [52], a study using 5-HT_{2C} knockout mice reported that the satiating effect of GLP-1 is blunted in the absence of 5-HT_{2C}

receptors [32]. However, the knockout study links GLP-1 receptor activation and 5-HT_{2C} receptors, not specifically 5-HT_{2C} receptors on PPG neurons. Furthermore, even if PPG neurons are involved, the effect of the loss of 5-HT_{2C} receptors may reside downstream, rather than upstream, from the PPG neurons.

The results discussed so far suggest an excitatory role for 5-HT_{2C} receptors on dendrites and a lack of propagation of the Ca^{2+} signal to somata, an effect that has been described previously for other central neurons, including neocortical and hippocampal pyramidal neurons [53,54]. A response to 5-HT that is confined to a specific subcellular

compartment could have several causes. We reject the hypothesis that 20 μM 5-HT could be subthreshold for activation of PPG neurons *in vitro* because increasing the concentration of 5-HT to 200 μM failed to elicit somatic responses and had no further effect on dendritic Ca^{2+} spiking. Alternatively, activation of 5-HT_{2C} receptors on dendrites would result in depolarization locally but failure of the signal to reach the soma due to simultaneous activation of inhibitory 5-HT receptors on the cell body. However, we can reject this scenario as well because we should have observed somatic Ca^{2+} increases upon selective activation of 5-HT_{2C} receptors using WAY161,503. In fact, 5-HT_{2C} receptor activation mimicked the response to 5-HT. We therefore propose that activation of 5-HT_{2C} receptors on PPG neurons leads to compartmentalized increases in Ca^{2+} in dendrites but not somata. Such local Ca^{2+} transients have previously been implicated in synaptic plasticity, enhancing somatic spike precision and dendritic release of neurotransmitters, including neuropeptides [53].

4.2. Inhibitory responses to 5-HT

Although optical recordings mainly revealed effects of 5-HT on dendritic Ca^{2+} spikes, our immunohistochemical results provide evidence for close appositions from 5-HT-containing axons not only onto distal dendrites but also onto somata and proximal dendrites. These observations suggest that PPG neurons are able to respond to 5-HT somatically in addition to the dendritic 5-HT_{2C} receptor-mediated Ca^{2+} spikes that we observed with optical recordings. With that possibility in mind, we performed cell-attached patch clamp recordings to explore both excitatory and inhibitory changes in firing frequency of spontaneously active PPG neurons upon exposure to 5-HT. The cell-attached firing rate was similar to that observed in perforated whole cell recordings in our earlier studies and changes in firing rate correlated with changes in intracellular Ca^{2+} [34,35]. Only a quarter of electrically recorded cells increased firing rate in response to 5-HT, in accordance with our finding that few PPG neurons showed an increase in somatic Ca^{2+} . More significantly, we observed that 5-HT application reduced electrical activity in almost half of the NTS PPG neurons tested. 5-HT-induced inhibition of firing rate was dependent on 5-HT_{1A} receptors that presumably occur on somata.

Interestingly, blocking the inhibitory response to 5-HT with WAY100,635 did not lead to excitation of PPG neurons by 5-HT. This finding has two possible explanations, which are not mutually exclusive. Firstly, the PPG neurons that exhibit dendritic calcium rises and the neurons in which somata are inhibited may belong to separate populations. Secondly, the pronounced dendritic activation observed in the presence of 5-HT does not lead to somatic and axonal activation, even when inhibitory 5-HT responses at the soma are blocked, because the dendritic compartment is functionally isolated from the soma, at least in respect to Ca^{2+} spikes. While we cannot determine whether the excitatory and inhibitory 5-HT responses occur on separate PPG neuron populations, the failure of the 5-HT_{2C} receptor agonist to produce somatic excitation, discussed in the previous section, strongly argues for compartmentalization of the dendritic calcium spikes.

4.3. Physiological significance

Our study has shown that 5-HT has two main effects on PPG neurons. First, it inhibits the electrical activity of approximately 50% of NTS PPG neurons via 5-HT_{1A} receptors. At the same time, 5-HT also produces significant activation of the dendritic compartment of PPG neurons via 5-HT_{2C} receptors. Both 5-HT_{1A} receptors and 5-HT_{2C} receptors have been implicated in the regulation of food intake. 5-HT_{1A} receptor blockade suppresses food intake [27], as disinhibition of PPG neurons

would do. In addition, loss of 5-HT_{2C} receptors produces hyperphagia [30], suggesting that 5-HT_{2C} receptor activation reduces appetite, as has been demonstrated for activation of PPG neurons [15]. Thus, the opposite effects of activation of these two types of 5-HT receptors on PPG neurons align with the physiological roles of these receptors.

It was beyond the scope of this study to determine the origin of the 5-HT-immunoreactive axons that appose PPG neurons. However, serotonergic axons from more than one CNS site, including the raphe magnus and obscurus but not the dorsal raphe nuclei, converge in the NTS [50,55]. A detailed anatomical dissection of the origin of individual serotonergic inputs may help explain the heterogeneous response to 5-HT observed in the current study and further clarify how serotonin modulates the activity of PPG neurons.

5. CONCLUSIONS

In the brain, both GLP-1 and 5-HT control a wide range of tightly-regulated homeostatic processes, including food intake and cardiovascular function. We have previously found that PPG neurons innervate 5-HT-containing neurons in the caudal raphe and show here that many PPG neurons in turn receive serotonergic innervation. However, cellular responses to 5-HT in PPG neurons were heterogeneous and compartmentalized. The firing rates of some PPG neurons increased upon 5-HT application while the firing rates of other PPG neurons decreased. In addition, distal dendrites showed transient Ca^{2+} spikes that failed to propagate to the soma. Identification of the 5-HT receptor types involved in these opposite responses, revealed that these receptors are also reported to have opposite effects on food intake, thus conforming to a role of GLP-1 as a satiety factor. The data reported here indicate that within the brain there are complex links between 5-HT and GLP-1 transmission, which are likely to be important for the regulation of satiety.

AUTHOR CONTRIBUTIONS

ST and ILS conceived the project. FR and FMG provided the transgenic mice. MKH performed the *in vitro* experiments. ILS performed the immunohistochemistry. ST and MKH wrote the manuscript and all authors contributed to editing and provided intellectual input.

ACKNOWLEDGMENTS

This study was supported by grants MR/J013293/2 from the MRC, UK (ST) and Project Grant #1025031 from NHMRC Australia (ILS). MKH holds a UCL Graduate Research Scholarship. FR and FMG are supported by the Wellcome Trust (106262/Z/14/Z, 106263/Z/14/Z) and the MRC (MRC_MC_UU_12012/3). We thank Prof Andy Ramage for valuable input on the design of this study.

CONFLICT OF INTEREST

The authors declare no potential conflict of interest.

REFERENCES

- [1] Holst, J.J., 2007. The physiology of glucagon-like peptide 1. *Physiological Reviews* 87:1409–1439.
- [2] Yamamoto, H., Lee, C.E., Marcus, J.N., Williams, T.D., Overton, J.M., Lopez, M.E., et al., 2002. Glucagon-like peptide-1 receptor stimulation increases blood pressure and heart rate and activates autonomic regulatory neurons. *Journal of Clinical Investigation* 110:43–52.
- [3] Ghosal, S., Myers, B., Herman, J.P., 2013. Role of central glucagon-like peptide-1 in stress regulation. *Physiology & Behavior* 122:201–207.

- [4] Gil-Lozano, M., Pérez-Tilve, D., Alvarez-Crespo, M., Martis, A., Fernandez, A.M., Catalina, P.A.F., et al., 2010. GLP-1(7-36)-amide and exendin-4 stimulate the HPA axis in rodents and humans. *Endocrinology* 151:2629–2640.
- [5] Robinson, L.E., Holt, T.A., Rees, K., Randeve, H.S., O'Hare, J.P., 2013. Effects of exenatide and liraglutide on heart rate, blood pressure and body weight: systematic review and meta-analysis. *BMJ Open* 3.
- [6] Ulrich-Lai, Y.M., Herman, J.P., 2009. Neural regulation of endocrine and autonomic stress responses. *Nature Reviews Neuroscience* 10:397–409.
- [7] Kreisler, A.D., Rinaman, L., 2016. Hindbrain glucagon-like peptide-1 neurons track intake volume and contribute to injection stress-induced hypophagia in meal-entrained rats. *American Journal of Physiology-Regulatory, Integrative and Comparative Physiology* 310:R906–R916.
- [8] Holt, M.K., Trapp, S., 2016. The physiological role of the brain GLP-1 system in stress. *Cogent Biology* 2:1229086.
- [9] Llewellyn-Smith, I.J., Reimann, F., Gribble, F.M., Trapp, S., 2011. Preproglucagon neurons project widely to autonomic control areas in the mouse brain. *Neuroscience* 180:111–121.
- [10] Merchenthaler, I., Lane, M., Shughrue, P., 1999. Distribution of pre-proglucagon and glucagon-like peptide-1 receptor messenger RNAs in the rat central nervous system. *Journal of Comparative Neurology* 403:261–280.
- [11] Larsen, P.J., Tang-Christensen, M., Holst, J.J., Orskov, C., 1997. Distribution of glucagon-like peptide-1 and other preproglucagon-derived peptides in the rat hypothalamus and brainstem. *Neuroscience* 77:257–270.
- [12] Trapp, S., Richards, J.E., 2013. The gut hormone glucagon-like peptide-1 produced in brain: is this physiologically relevant? *Current Opinion in Pharmacology* 13:964–969.
- [13] Vrang, N., Phifer, C.B., Corkern, M.M., Berthoud, H.R., 2003. Gastric distension induces c-Fos in medullary GLP-1/2-containing neurons. *American Journal of Physiology. Regulatory, Integrative and Comparative Physiology* 285:R470–R478.
- [14] Rinaman, L., 1999. Interoceptive stress activates glucagon-like peptide-1 neurons that project to the hypothalamus. *American Journal of Physiology* 277:R582–R590.
- [15] Gaykema, R.P., Newmyer, B.A., Ottolini, M., Rajee, V., Warthen, D.M., Lambeth, P.S., et al., 2017. Activation of murine pre-proglucagon-producing neurons reduces food intake and body weight. *Journal of Clinical Investigation* 127:1031–1045.
- [16] Llewellyn-Smith, I.J., Marina, N., Manton, R.N., Reimann, F., Gribble, F.M., Trapp, S., 2015. Spinally projecting preproglucagon axons preferentially innervate sympathetic preganglionic neurons. *Neuroscience* 284:872–887.
- [17] Cork, S.C., Richards, J.E., Holt, M.K., Gribble, F.M., Reimann, F., Trapp, S., 2015. Distribution and characterisation of glucagon-like peptide-1 receptor expressing cells in the mouse brain. *Molecular Metabolism* 4:718–731.
- [18] Turton, M.D., O'Shea, D., Gunn, I., Beak, S.A., Edwards, C.M., Meeran, K., et al., 1996. A role for glucagon-like peptide-1 in the central regulation of feeding. *Nature* 379:69–72.
- [19] Griffioen, K.J., Wan, R., Okun, E., Wang, X., Lovett-Barr, M.R., Li, Y., et al., 2011. GLP-1 receptor stimulation depresses heart rate variability and inhibits neurotransmission to cardiac vagal neurons. *Cardiovascular Research* 89:72–78.
- [20] Lockie, S.H., Heppner, K.M., Chaudhary, N., Chabenne, J.R., Morgan, D.A., Veyrat-Durebex, C., et al., 2012. Direct control of brown adipose tissue thermogenesis by central nervous system glucagon-like peptide-1 receptor signaling. *Diabetes* 61:2753–2762.
- [21] Trapp, S., Hisadome, K., 2011. Glucagon-like peptide 1 and the brain: central actions-central sources? *Autonomic Neuroscience* 161:14–19.
- [22] Heisler, L.K., Zhou, L., Bajwa, P., Hsu, J., Tecott, L.H., 2007. Serotonin 5-HT(2C) receptors regulate anxiety-like behavior. *Genes, Brain, and Behavior* 6:491–496.
- [23] Heisler, L.K., Cowley, M.A., Kishi, T., Tecott, L.H., Fan, W., Low, M.J., et al., 2003. Central serotonin and melanocortin pathways regulating energy homeostasis. *Annals of the New York Academy of Sciences* 994:169–174.
- [24] Heisler, L.K., Chu, H.M., Brennan, T.J., Danao, J.A., Bajwa, P., Parsons, L.H., et al., 1998. Elevated anxiety and antidepressant-like responses in serotonin 5-HT1A receptor mutant mice. *Proceedings of the National Academy of Sciences of the United States of America* 95:15049–15054.
- [25] Li, B., Shao, D., Luo, Y., Wang, P., Liu, C., Zhang, X., et al., 2015. Role of 5-HT3 receptor on food intake in fed and fasted mice. *PLoS One* 10:e0121473.
- [26] Vickers, S.P., Clifton, P.G., Dourish, C.T., Tecott, L.H., 1999. Reduced satiating effect of d-fenfluramine in serotonin 5-HT(2C) receptor mutant mice. *Psychopharmacology (Berl)* 143:309–314.
- [27] Dill, M.J., Shaw, J., Cramer, J., Sindelar, D.K., 2013. 5-HT1A receptor antagonists reduce food intake and body weight by reducing total meals with no conditioned taste aversion. *Pharmacology Biochemistry and Behavior* 112:1–8.
- [28] Kennett, G.A., Dourish, C.T., Curzon, G., 1987. 5-HT1B agonists induce anorexia at a postsynaptic site. *European Journal of Pharmacology* 141:429–435.
- [29] Tecott, L.H., Sun, L.M., Akana, S.F., Strack, A.M., Lowenstein, D.H., Dallman, M.F., et al., 1995. Eating disorder and epilepsy in mice lacking 5-HT2C serotonin receptors. *Nature* 374:542–546.
- [30] Nonogaki, K., Strack, A.M., Dallman, M.F., Tecott, L.H., 1998. Leptin-independent hyperphagia and type 2 diabetes in mice with a mutated serotonin 5-HT2C receptor gene. *Natural Medicines* 4:1152–1156.
- [31] Nonogaki, K., Suzuki, M., Sanuki, M., Wakameda, M., Tamari, T., 2011. The contribution of serotonin 5-HT2C and melanocortin-4 receptors to the satiety signaling of glucagon-like peptide 1 and liraglutide, a glucagon-like peptide 1 receptor agonist, in mice. *Biochemical and Biophysical Research Communications* 411:445–448.
- [32] Asarian, L., 2009. Loss of cholecystokinin and glucagon-like peptide-1-induced satiation in mice lacking serotonin 2C receptors. *American Journal of Physiology-Regulatory, Integrative and Comparative Physiology* 296:R51–R56.
- [33] Llewellyn-Smith, I.J., Gnanamanickam, G.J., Reimann, F., Gribble, F.M., Trapp, S., 2013. Preproglucagon (PPG) neurons innervate neurochemically identified autonomic neurons in the mouse brainstem. *Neuroscience* 229:130–143.
- [34] Hisadome, K., Reimann, F., Gribble, F.M., Trapp, S., 2011. CCK Stimulation of GLP-1 neurons involves α 1-adrenoceptor-mediated increase in glutamatergic synaptic inputs. *Diabetes* 60:2701–2709.
- [35] Hisadome, K., Reimann, F., Gribble, F.M., Trapp, S., 2010. Leptin directly depolarizes preproglucagon neurons in the nucleus tractus solitarius: electrical properties of glucagon-like Peptide 1 neurons. *Diabetes* 59:1890–1898.
- [36] Tian, L., Hires, S.A., Looger, L.L., 2012. Imaging neuronal activity with genetically encoded calcium indicators. *Cold Spring Harbor Protocols* 2012:647–656.
- [37] Anesten, F., Holt, M.K., Schele, E., Palsdottir, V., Reimann, F., Gribble, F.M., et al., 2016. Preproglucagon neurons in the hindbrain have IL-6 receptor-alpha and show Ca^{2+} influx in response to IL-6. *American Journal of Physiology-Regulatory, Integrative and Comparative Physiology* 311:R115–R123.
- [38] Tian, L., Hires, S.A., Mao, T., Huber, D., Chiappe, M.E., Chalasani, S.H., et al., 2009. Imaging neural activity in worms, flies and mice with improved GCaMP calcium indicators. *Nature Methods* 6:875–881.
- [39] Reimann, F., Habib, A.M., Tolhurst, G., Parker, H.E., Rogers, G.J., Gribble, F.M., 2008. Glucose sensing in L cells: a primary cell study. *Cell Metabolism* 8:532–539.
- [40] Parker, H.E., Adriaenssens, A., Rogers, G., Richards, P., Koepsell, H., Reimann, F., et al., 2012. Predominant role of active versus facilitative glucose transport for glucagon-like peptide-1 secretion. *Diabetologia* 55:2445–2455.
- [41] Llewellyn-Smith, I.J., Dicarlo, S.E., Collins, H.L., Keast, J.R., 2005. Enkephalin-immunoreactive interneurons extensively innervate sympathetic preganglionic neurons regulating the pelvic viscera. *Journal of Comparative Neurology* 488:278–289.

- [42] Machhada, A., Ang, R., Ackland, G.L., Ninkina, N., Buchman, V.L., Lythgoe, M.F., et al., 2015. Control of ventricular excitability by neurons of the dorsal motor nucleus of the vagus nerve. *Heart Rhythm* 12:2285–2293.
- [43] Schindelin, J., Arganda-Carreras, I., Frise, E., Kaynig, V., Longair, M., Pietzsch, T., et al., 2012. Fiji: an open-source platform for biological-image analysis. *Nature Methods* 9:676–682.
- [44] Thevenaz, P., Ruttimann, U.E., Unser, M., 1998. A pyramid approach to subpixel registration based on intensity. *IEEE Transactions on Image Processing: a Publication of the IEEE Signal Processing Society* 7:27–41.
- [45] Balkenius, A., Johansson, A.J., Balkenius, C., 2015. Comparing analysis methods in functional calcium imaging of the insect brain. *PLoS One* 10:e0129614.
- [46] Jordan, D., 2005. Vagal control of the heart: central serotonergic (5-HT) mechanisms. *Experimental Physiology* 90:175–181.
- [47] Wang, Y., Ramage, A.G., Jordan, D., 1997. In vivo effects of 5-hydroxytryptamine receptor activation on rat nucleus tractus solitarius neurones excited by vagal C-fibre afferents. *Neuropharmacology* 36:489–498.
- [48] McCorvy, J.D., Roth, B.L., 2015. Structure and function of serotonin G protein-coupled receptors. *Pharmacology & Therapeutics* 150:129–142.
- [49] Cui, R.J., Roberts, B.L., Zhao, H., Zhu, M., Appleyard, S.M., 2012. Serotonin activates catecholamine neurons in the solitary tract nucleus by increasing spontaneous glutamate inputs. *Journal of Neuroscience* 32:16530–16538.
- [50] Wu, Q., Clark, M.S., Palmiter, R.D., 2012. Deciphering a neuronal circuit that mediates appetite. *Nature* 483:594–597.
- [51] Lam, D.D., Przydzial, M.J., Ridley, S.H., Yeo, G.S., Rochford, J.J., O'Rahilly, S., et al., 2008. Serotonin 5-HT_{2C} receptor agonist promotes hypophagia via downstream activation of melanocortin 4 receptors. *Endocrinology* 149:1323–1328.
- [52] Lam, D.D., Zhou, L., Vegge, A., Xiu, P.Y., Christensen, B.T., Osundiji, M.A., et al., 2009. Distribution and neurochemical characterization of neurons within the nucleus of the solitary tract responsive to serotonin agonist-induced hypophagia. *Behavioural Brain Research* 196:139–143.
- [53] Sjostrom, P.J., Rancz, E.A., Roth, A., Hausser, M., 2008. Dendritic excitability and synaptic plasticity. *Physiological Reviews* 88:769–840.
- [54] Jarsky, T., Roxin, A., Kath, W.L., Spruston, N., 2005. Conditional dendritic spike propagation following distal synaptic activation of hippocampal CA1 pyramidal neurons. *Nature Neuroscience* 8:1667–1676.
- [55] Thor, K.B., Helke, C.J., 1987. Serotonin- and substance P-containing projections to the nucleus tractus solitarii of the rat. *Journal of Comparative Neurology* 265:275–293.